Earthquakes and Structures, *Vol. 4, No. 5 (2013) 557-585*
DOI: http://dx.doi.org/10.12989/eas.2013.4.5.557

Occurrence mechanism of recent large earthquake ground motions at nuclear power plant sites in Japan under soil-structure interaction

Shuichi KAMAGATA[1] and Izuru TAKEWAKI[*2]

[1]*Nuclear Power Department, Kajima Corporation, Tokyo 107-8348, Japan*
[2]*Dept of Architecture and Architectural Eng., Kyoto University, Kyoto 615-8540, Japan*

(Received September 10, 2012, Revised December 20, 2012, Accepted January 3, 2013)

Abstract. The recent huge earthquake ground motion records in Japan result in the reconsideration of seismic design forces for nuclear power stations from the view point of seismological research. In addition, the seismic design force should be defined also from the view point of structural engineering. In this paper it is shown that one of the occurrence mechanisms of such large acceleration in recent seismic records (recorded in or near massive structures and not free-field ground motions) is due to the interaction between a massive building and its surrounding soil which induces amplification of local mode in the surface soil. Furthermore on-site investigation after earthquakes in the nuclear power stations reveals some damages of soil around the building (cracks, settlement and sand boiling). The influence of plastic behavior of soil is investigated in the context of interaction between the structure and the surrounding soil. Moreover the amplification property of the surface soil is investigated from the seismic records of the Suruga-gulf earthquake in 2009 and the 2011 off the Pacific coast of Tohoku earthquake in 2011. Two methods are introduced for the analysis of the non-stationary process of ground motions. It is shown that the non-stationary Fourier spectra can detect the temporal change of frequency contents of ground motions and the displacement profile integrated from its acceleration profile is useful to evaluate the seismic behavior of the building and the surrounding soil.

Keywords: large acceleration; pulse wave; non-linear behavior; soil-structure interaction; settlement; non-stationary Fourier spectra; frequency component ratio; surface soil amplification; occurrence mechanism of pulse wave; amplification factor

1. Introduction

Three major earthquakes occurred in Japan every two years recently (2007, 2009, 2011) and they stopped the operation of nuclear power stations (NPS). Unexpectedly large acceleration records were observed and brought many discussions (for example see Yamada *et al.* 2009, 2010, Takewaki 2011, Takabatake and Matsuoka 2012). These records are different from those found in previous studies of near-fault ground motions (see Kamae *et al.* 2004, Tothong and Cornell 2008, Yang *et al.* 2009, Tahghighi 2011, Jayaram *et al.* 2011). The Niigata-ken Chuetsu-oki earthquake in 2007 occurred near the Kashiwazaki-Kariwa NPS and the Suruga-gulf earthquake in 2009

[*]Corresponding author, Professor, E-mail: takewaki@archi.kyoto-u.ac.jp

Copyright © 2013 Techno-Press, Ltd.
http://www.techno-press.org/?journal=eas&subpage=7 ISSN: 2092-7614 (Print), 2092-7622 (Online)

Fig. 1 Earthquake events and location of nuclear power stations (Produced using Google Maps API (http ://www5.ocn.ne.jp/~botan/map_g.html))

Table 1 Seismic events

Seismic event	Origin time	Magnitude	Latitude	Longitude
Niigata-ken Chuetsu-oki	2007/07/16	*M*6.8	37.56 N	138.61E
Suruga-gulf	2009/08/11	*M*6.5	34.78 N	138.50E
Off the Pacific coast of Tohoku	2011/03/11	*M*9.0	38.16 N	142.86E

occurred near the Hamaoka NPS. Most recently the 2011 off the Pacific coast of Tohoku earthquake occurred near the Fukushima-daiichi NPS, the Fukusima-daini NPS and Onagawa NPS (see Fig. 1).

In the seismic records of Kashiwazaki-Kariwa NPS (see Tokyo Electric Power Company 2007), the maximum acceleration record at the foundation of the No.1-unit reactor building is 680 cm/s^2, which exceeds two and half times of the design value. The variance of the maximum accelerations from No. 1-unit to No. 7-unit is too large to evaluate the occurrence mechanism (see Fig. 2). Consequently it has been explained that the seismic fault and the soil properties in the propagation path caused the variance (see Japan Nuclear Energy Safety Organization 2008).

In the seismic records at the Hamaoka NPS during the Suruga-gulf earthquake in 2009 (see Chubu Electric Power Company 2009), the maximum acceleration at the foundation of the No.5-unit reactor building is 438 cm/s^2, which exceeds more than two times of the maximum accelerations of other units (see Fig. 3). It is shown that the occurrence mechanism of the variance results from the soil property in the propagation path from the epicenter to the reactor building.

The third earthquake is the historically huge earthquake and the moment magnitude (Mw=9.0) is related to the existence of multi-faults. The earthquake attacked three NPSs, i.e., Fukusima-daiichi NPS, Fukusima-daini NPS, and Onagawa NPS. Finally the tsunami after the earthquake attacked the nuclear power stations, caused the station black out, and melted-down the nuclear reactor of Fukushima-daiichi NPS.

The purpose of this paper is to make clear the occurrence mechanism of the large acceleration

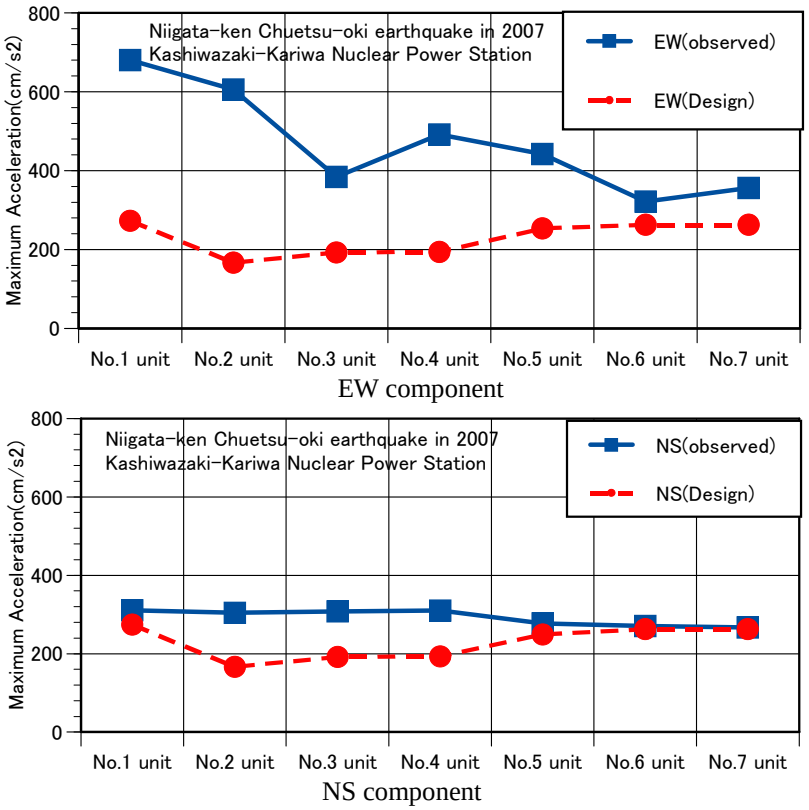

Fig. 2 Observed maximum accelerations and design values (Kashiwazaki-Kariwa NPS during the earthquake in 2007)

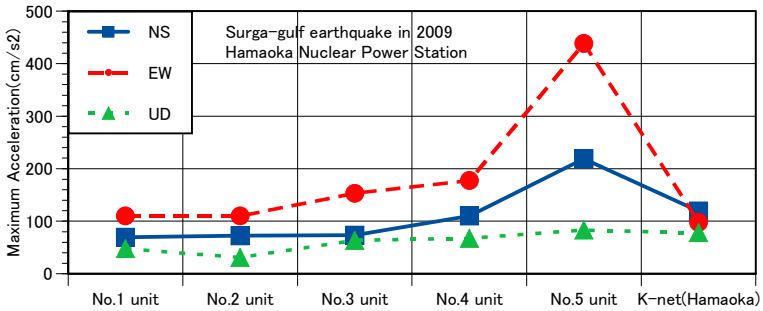

Fig. 3 Maximum accelerations at Hamaoka NPS during the Suruga-gulf earthquake in 2009

in the recent seismic records. The seismic behavior of a building and its surrounding soil is investigated by means of the non-stationary Fourier spectra and the numerically integrated displacement profile. The seismic records at the Kashiwazaki-Kariwa NPS during the Niigata-ken Chuetsu-oki earthquake in 2007 are analyzed to investigate the interaction between the building and the surrounding soil. Many seismic recorders are set in the NPS as the high density seismic array system, also the seismic records from the Strong-motion Seismograph Networks (KiK-net) are utilized to investigate the amplification effect of surface soil. This is done also for the seismic

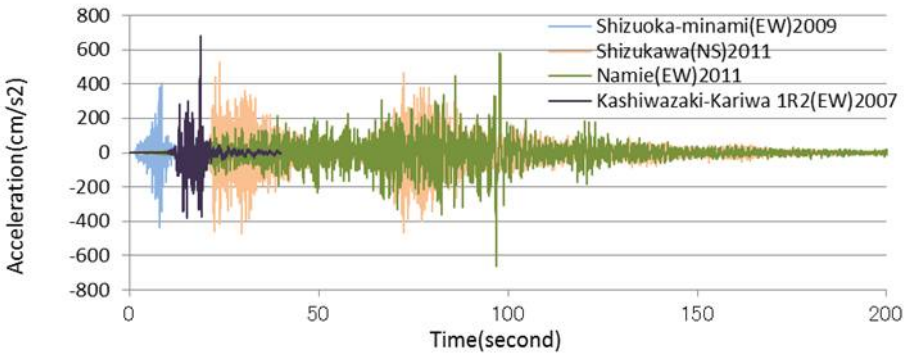

Fig.4 Acceleration records from three seismic events

records during the Suruga-gulf earthquake in 2009 and the 2011 off the Pacific coast of Tohoku earthquake.

In Fig. 4, four seismic records are compared, namely the Shizuoka-minami (EW) is selected from KiK-net seismography of the Suruga-gulf earthquake in 2009, Shizukawa (NS) and Namie (EW) are selected from KiK-net seismography of the 2011 off the Pacific coast of Tohoku earthquake, and Kashiwazaki-Kariwa 1R2 (EW) is selected from the seismic record of Niigata-ken Chuetsu-oki earthquake in 2007 (Japan Association for Earthquake Engineering). The duration time of the 2011 off the Pacific coast of Tohoku earthquake was more than two minutes, which may result from the multi-faults. In the selected four seismic records, the maximum value of the acceleration was measured at the Kashiwazaki-Kariwa NPS.

2. The Niigata-ken Chuetsu-oki earthquake in 2007

The Niigata-ken Chuetsu-oki earthquake in 2007 raised the need of re-evaluation of the seismic design method for the nuclear equipment facilities because the measured maximum acceleration exceeded the design value. The investigation on the seismic event was conducted mainly from the seismological viewpoint such as the asperity of the fault (see Japan Nuclear Energy Safety Organization 2008). While Trifunac introduced the response envelope spectra as running spectra (Trifunac 1971), Kamagata developed the non-stationary Fourier spectra to evaluate the non-stationary property of seismic records (Kamagata 1991). In addition to the seismic records with large acceleration value, the settlement more than one meter was observed between the structure and the surrounding soil. The interaction between the structure and the surrounding soil was then investigated.

2.1 Property of pulse wave in seismic record (see Japan Nuclear Energy Safety Organization 2009, Kamagata 2009)

Although the maximum acceleration of 680 cm/s^2 at the foundation of No. 1 unit nuclear reactor building (1R2) occurred around 10 seconds, the dominant component did not occur at the seismic record of the service hall (SG3) (see Fig. 5).

From the non-stationary Fourier spectra shown in Fig. 5, the following information is obtained.

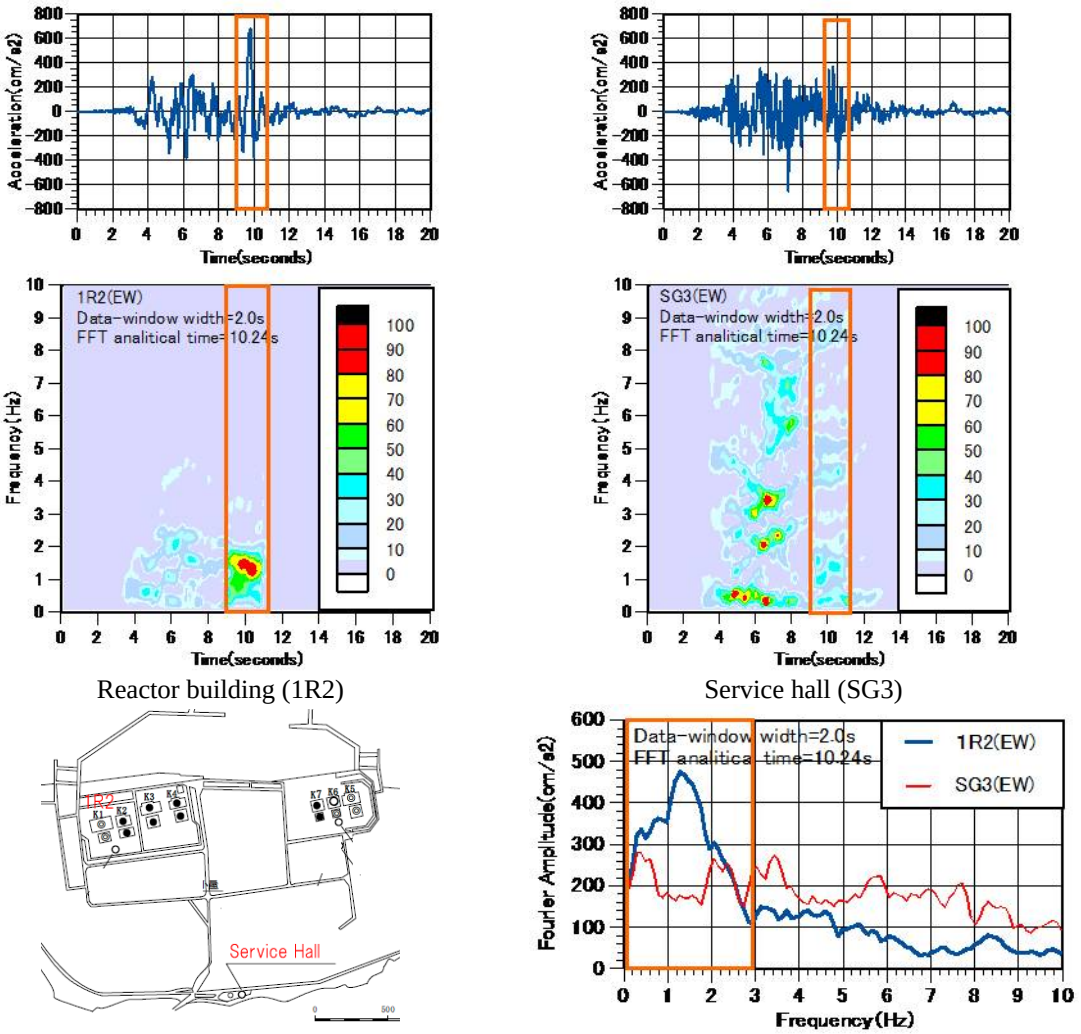

Fig. 5 Non-stationary Fourier spectra and Fourier amplitude of 1R2 (EW) and SG3 (EW)

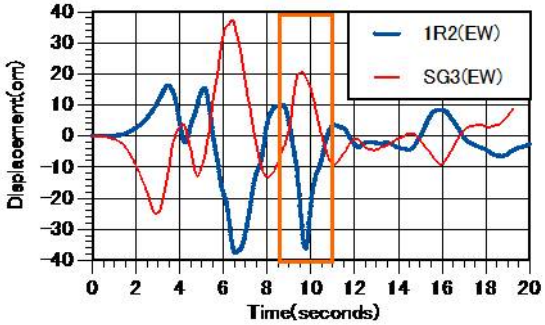

Fig. 6 Displacement profile of reactor building (1R2) and service hall (SG3)

The dominant component of the 1R2 (EW) has the frequency of 1.4 Hz and the amplitude of

470 cm/s^2 around 10 seconds. The dominant components of the SG3 (EW) scattered at the frequency from 2.5 Hz to 5.0 Hz around the time from 4 seconds to 8 seconds. In the displacement profile shown in Fig. 6, the phase of the 1R2 (EW) and SG3 (EW) are different by π. From the 1R2 (EW), the shape of the second cycle around 10 seconds is sharper than that of the first cycle around from 6 to 7 seconds.

2.2 Identification of pulse wave by Ricker wavelet

From the comparison of the recorded acceleration profile and the integrated displacement profile, the pulse wave at 1R2 (EW) was found to be related to the second cycle of the displacement profile as shown in Fig. 7. The non-stationary Fourier spectra indicate that the dominant frequency is 1.2 Hz and the maximum Fourier amplitude is 470 cm/s^2. Judging from the resemblance of wave-shapes, the Ricker wavelet was introduced to identify the pulse wave which caused the maximum acceleration (see Fig. 8).

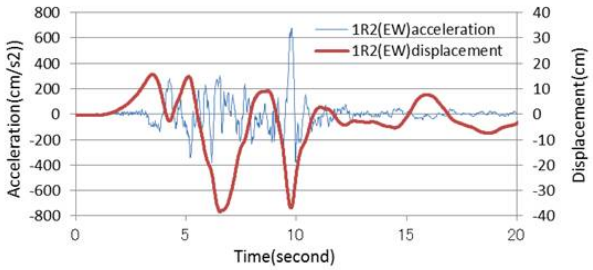

Fig. 7 Acceleration and displacement profiles at 1R2 (EW)

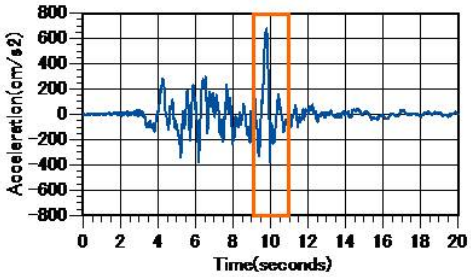

Ground acceleration at 1R2 (EW)

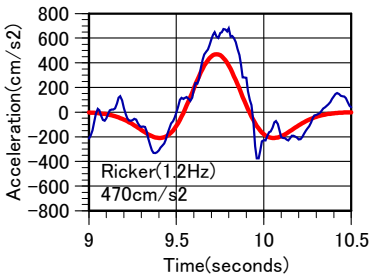

Identification by Ricker wavelet

Fig. 8 Identification of pulse wave by Ricker wavelet

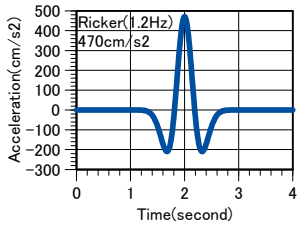

Acceleration

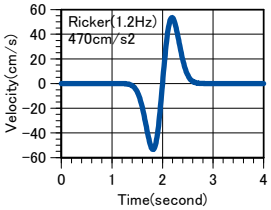

Velocity

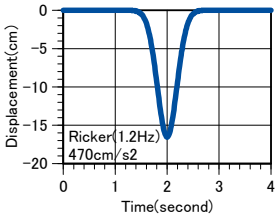

Displacement

Fig. 9 Acceleration, velocity and displacement profiles of Ricker wavelet

By means of the numerical integration, the acceleration profile identified using the Ricker wavelet was transformed to the velocity and displacement profiles (see Fig. 9). It was found that the displacement profile of the Ricker wavelet, exhibiting a one-sided shape with the amplitude of 16cm, is coincident with the shape of the measured record (see Japan Nuclear Energy Safety Organization 2009, Kamagata 2009).

2.3 Investigation on seismic behavior by field-survey after the earthquake

The nuclear power stations from No. 1 unit to No. 4 unit are located at the Arahama-site and their displacement profiles are almost similar as shown in Fig. 10. In the on-site investigation (see Tokyo Electric Power Company 2008), many cracks were detected on the ground surface, especially on the land-side near the reactor building of No. 1 unit. Furthermore the settlement of the soil around the building was detected.

From the displacement profile and the on-site investigation (see Fig. 11), it was found that the plastic deformation in the surrounding soil causing the pulse wave and the amplification of acceleration may be the principal occurrence mechanisms of the maximum acceleration (see Fig. 12).

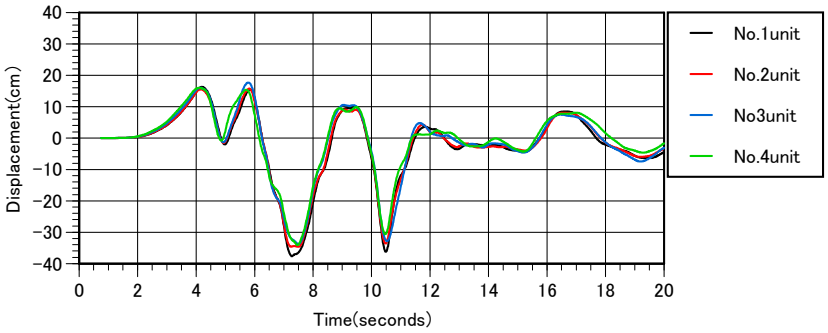

Fig. 10 Displacement profiles of four reactor buildings at Arahama-site

Fig. 11 On-site investigation after the earthquake

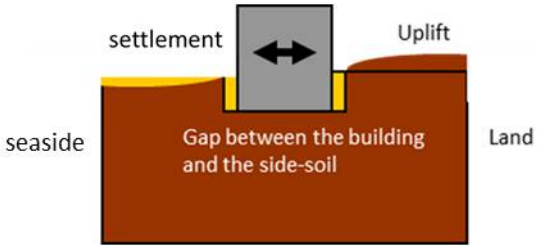

Fig. 12 Interaction between building and surrounding soil

2.4 Rocking mode induced by interaction between building and surrounding soil

Comparing the EW and UD components of the seismic records (see Figs. 13 and 14), it was found that the pulse wave of the UD component occurred just after the pulse wave of the EW component.

To make clear the relation of the EW and UD components, the displacement of the UD component was subdivided into four parts, namely the first part is before the first pulse wave, the second part covers the first pulse wave, the third part covers the second pulse wave and the fourth part is after the second pulse wave (see Fig. 15).

The orbits of the EW and UD displacements are illustrated in Fig. 16.

In the third part, the UD displacement shifts from -5 cm to 3 cm and the EW displacement shifts from -5 cm to zero. Moreover the EW displacement shifts to -32 cm without the change of the UD displacement. The pulse wave of the amplitude 680 cm/s^2 occurred in this process.

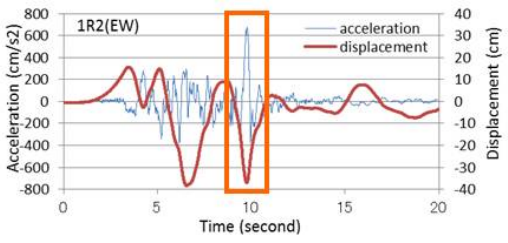

EW component

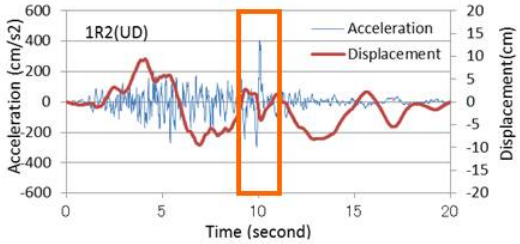

UD component

Fig. 13 Acceleration and displacement profiles

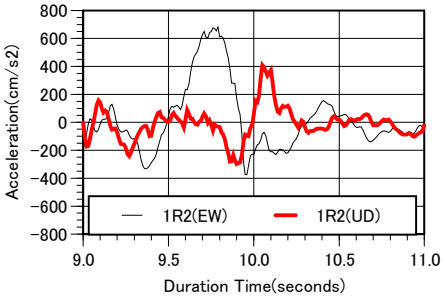

Fig. 14 Acceleration profile

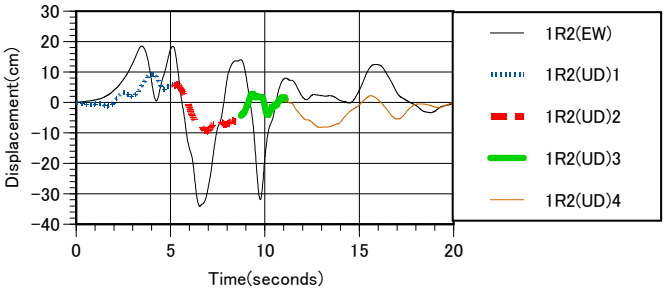

Fig. 15 Displacement profile

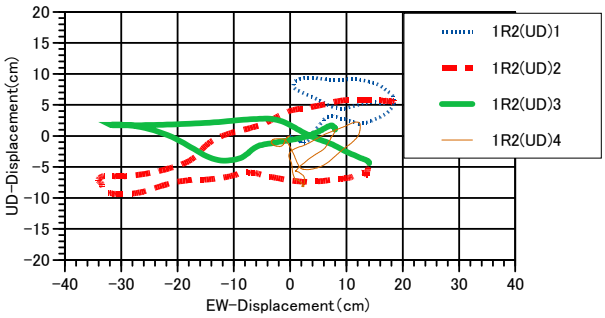

Fig. 16 Orbits of EW and UD displacements

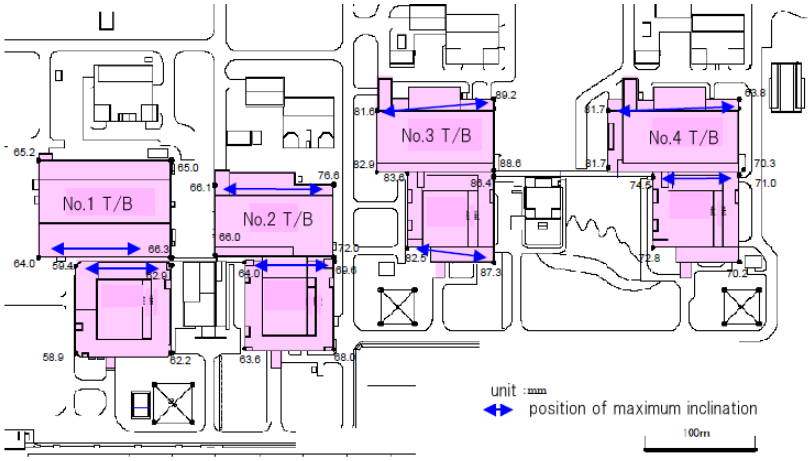

Fig. 17 Inclination of foundation after the earthquake

Comparing the peak-to-peak displacements of the UD component, it was found that the amplitude of the first pulse wave is 15 cm and that of the second pulse wave is 8 cm (Japan Nuclear Energy Safety Organization 2009, Kamagata 2009). The second pulse wave seems to have been caused as the movement of soil in the plastic region deteriorated in the first deformation.

The plastic deformation in the surrounding soil was observed as the inclination of the foundation, which is different from the measured value in February 2008 and May 2006. (see Fig. 17). The maximum residual inclination in the No. 1-unit reactor building occurred near the turbine building and the uplift value is 5.94 cm at the north-west corner and 6.29 cm at the north-east corner. The peak-to-peak amplitude of the integrated displacement corresponds to the maximum residual inclination.

As another possibility, the high peak ground motions can be as well due to the directivity pulses in the forward direction of rupture propagation as well as the source-to-receiver geometry. Further investigation will be necessary.

3. Amplification mechanism of acceleration in surface soil

For the Suruga-gulf earthquake in 2009 and the 2011 off the Pacific coast of Tohoku

Table 2 Maximum accelerations at surface and in borehole (cm/s^2)

	Surface			Borehole		
	NS	EW	UD	NS	EW	UD
Shizuoka-minami	429.0	431.6	246.0	104.6	87.4	67.2
Hukuroi	86.9	100.3	36.7	25.2	27.7	20.0
Shizukawa	526.5	459.8	264.9	156.9	241.4	112.6
Namie	394.1	660.5	266.3	157.5	356.4	154.6

Fig. 18 Soil condition and KiK-net record site (Produced using Google Maps API (http://www5.ocn.ne.jp/~botan/map_g.html))

earthquake, the seismic records from the KiK-net have been analyzed to make clear the amplification mechanism of acceleration in the surface soil. Since the KiK-net supplies the seismic records at the surface and in the borehole, they are useful to investigate the seismic behavior of surface soils.

3.1 Seismic data of KiK-net

In the seismic records of the Suruga-gulf earthquake in 2009, the records of Shizuoka-minami (SZOH33) and Hukuroi (SZOH26) are selected. The records of Shizukawa (MYGH12) and Namie (FKSH20) are also selected from the seismic records of the 2011 off the Pacific coast of Tohoku earthquake.

The maximum values of acceleration are shown in Table 2.

The profile of shear wave velocity and the site locations including the neighboring NPS are illustrated in Fig. 18. The comparison of accelerations at the surface and in the borehole is illustrated in Figs. 19 and 20. As for the 2011 off the Pacific coast of Tohoku earthquake, the seismic records are subdivided into two parts, as shown in Fig. 20, to evaluate the difference of the first and second main shocks.

3.2 Non-stationary Fourier spectra

The non-stationary Fourier spectra of the EW components at the Hukuroi 2009 and Shizuoka-minami 2009 are illustrated in Fig. 21, from which the dominant frequency component and the occurrence time of dominant components can be investigated. The Fourier amplitude is

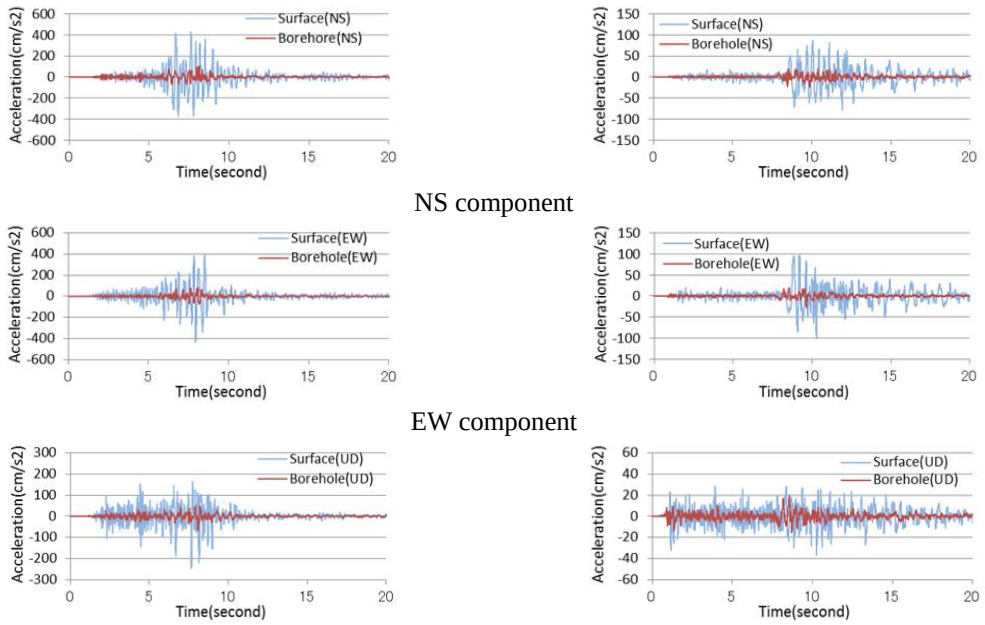

NS component

EW component

Hukuroi Shizuoka-minami

UD component

Fig. 19 Acceleration records during Suruga-gulf earthquake in 2009

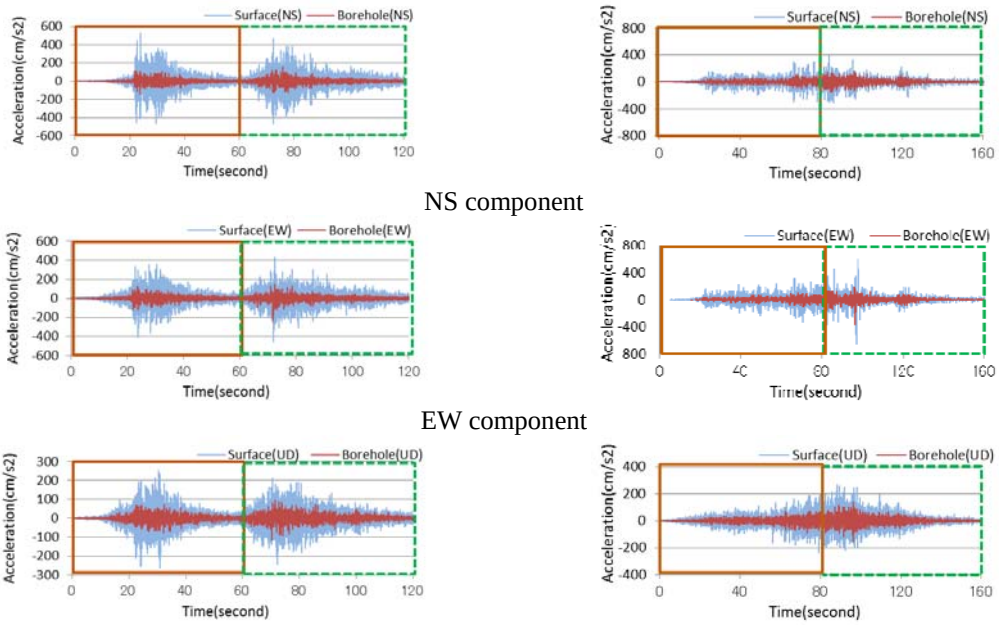

NS component

EW component

Shizukawa Namie

UD component

Fig. 20 Acceleration records during the 2011 off the Pacific coast of Tohoku earthquake

illustrated as a contour with 10 divisions. The maximum value of the Fourier amplitude in the duration time is shown as the Fourier amplitude.

$F_{RF}^{SF}(\omega_i; T_j)$; Non-stationary Fourier spectra at surface $(T_j; j = 1,2,\cdots M)$

$F_{RF}^{BH}(\omega_i; T_j)$; Non-stationary Fourier spectra in borehole $(T_j; j = 1,2,\cdots M)$

$F_{RF,MAX}^{SF}(\omega_i)$: Maximum value of $F_{RF}^{SF}(\omega_i; T_j)$ in duration time $(T_j; j = 1,2,\cdots M)$

$F_{RF,MAX}^{BH}(\omega_i)$: Maximum value of $F_{RF}^{BH}(\omega_i; T_j)$ in duration time $(T_j; j = 1,2,\cdots M)$

$M = T/\Delta T$ T ; Duration time of the seismic record

ΔT ; Time interval of FFT analysis

As for the seismic record at the Hukuroi (EW), the maximum Fourier amplitude at the surface is observed at 2.4 Hz with the value of 80 cm/s^2. On the other hand, the Fourier amplitude in the borehole is uniformly distributed with the value of 10 cm/s^2.

As for the seismic record of Shizuoka-minami (EW), the maximum Fourier amplitude at the surface is observed at 3.1 Hz with the value of 360 cm/s^2. On the other hand, the Fourier amplitude in the borehole is uniformly distributed with the value of 50 cm/s^2.

The seismic records at the surface include the amplified component dependent on the surface soil condition and the seismic records in the borehole have a uniformly distributed component.

3.3 Comparison of Fourier amplitudes and amplification factors

In order to evaluate the amplification property of the surface soil, the amplification factor is newly introduced as follows.

Amplification factor:

Maximum value of $F_{RF,MAX}^{SF}(\omega_i) / F_{RF,MAX}^{BH}(\omega_i)$ (i = 1, 2, …, N/2)

(1) Suruga-gulf earthquake in 2009

To compare the Fourier amplitudes and the amplification factors, they are illustrated in the same figure. The Fourier amplitude is illustrated as a thin line and the amplification factor is illustrated as a thick line in Fig. 22.

The Fourier amplitude at the surface is amplified in a wide frequency range less than 10 Hz and the magnitude of the amplification factor exceeds 10.0. The frequency of the maximum amplification factor is not necessarily the same with the frequency of the maximum Fourier amplitude.

(2) The 2011 off the Pacific coast of Tohoku earthquake

The Fourier amplitude of the EW component is illustrated in Fig. 23. Regarding the seismic records at Shizukawa, the Fourier amplitude in the borehole is almost coincident with the Fourier amplitude at the surface in the frequency range less than 2 Hz, which is related to the same phase of the displacement profile. The amplification factor becomes greater with the increase of the frequency.

The Fourier amplitude at the surface has the dominant frequency of 0.6 Hz (640 cm/s^2), and the Fourier amplitude in the borehole has the dominant frequency of 0.7 Hz (170 cm/s^2). The maximum amplification factor is 6.7 at the frequency of 1.7 Hz. The amplification factor is larger in the frequency range less than 5 Hz.

3.4 Frequency component ratio

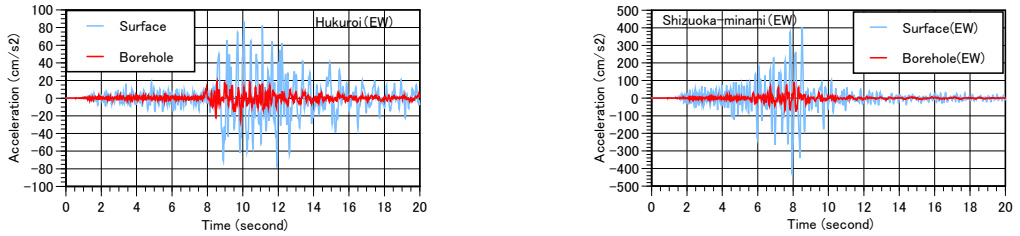

Acceleration profile (surface and borehole)

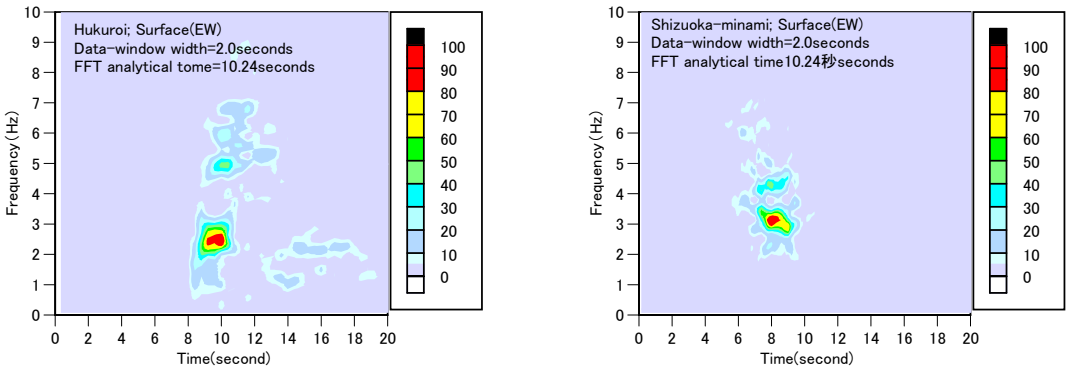

Surface

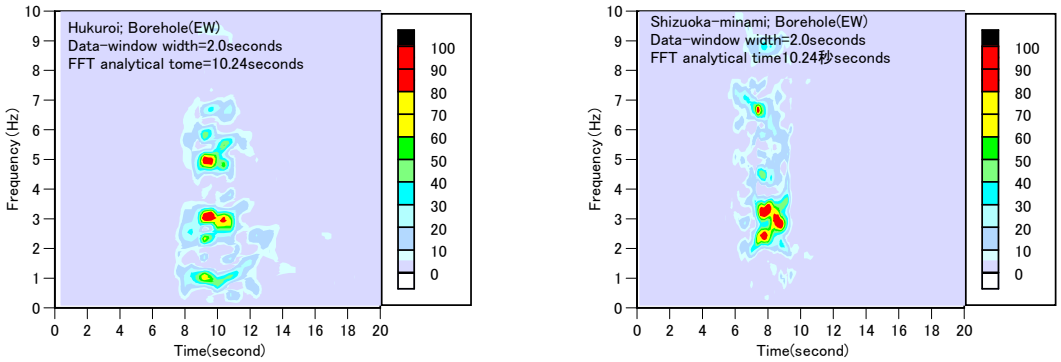

Borehole

Non-stationary Fourier spectra

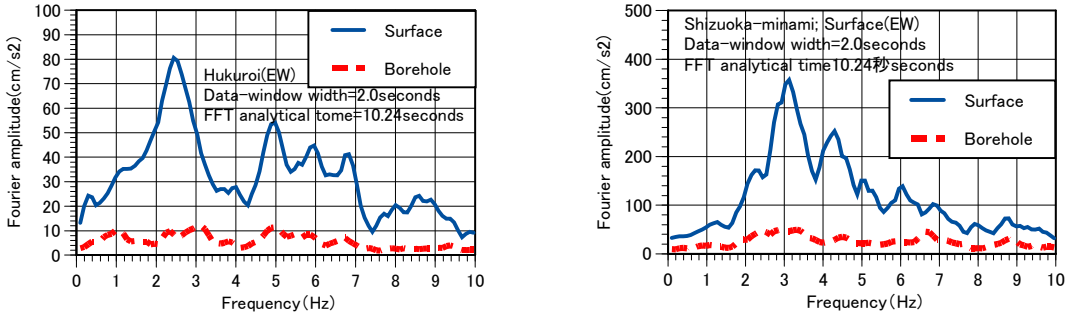

Fourier spectra (surface and borehole)

Hukuroi (EW) Shizuoka-minami (EW)

Fig. 21 Acceleration profile, non-stationary Fourier spectra and Fourier spectra during Suruga-gulf earthquake in 2009

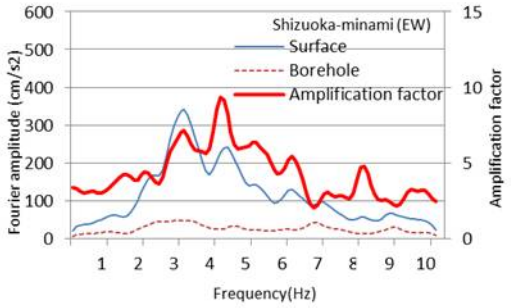

Shizuoka-minami (EW) 2009

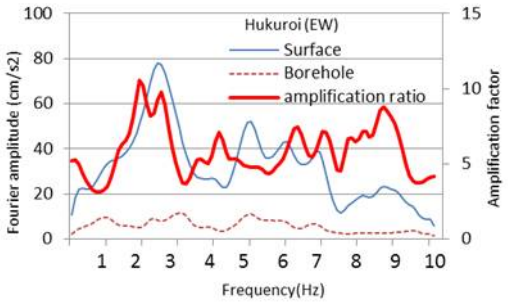

Hukuroi (EW) 2009

Fig. 22 Fourier amplitude and amplification factor during Suruga-gulf earthquake in 2009

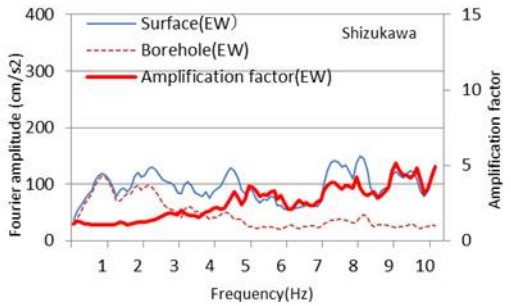

Shizukawa (EW) 2009

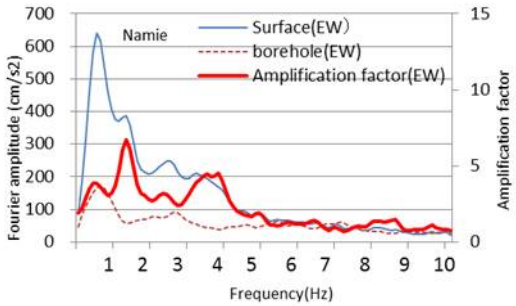

Namie (EW) 2009

Fig. 23 Fourier amplitude and amplification factor during the 2011 off the Pacific coast of Tohoku earthquake

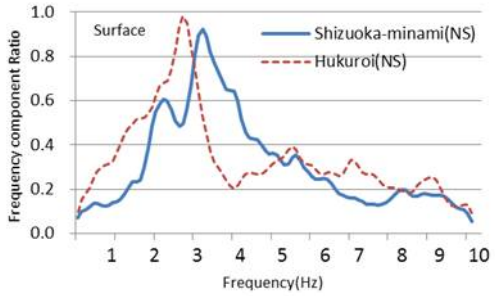

Surface

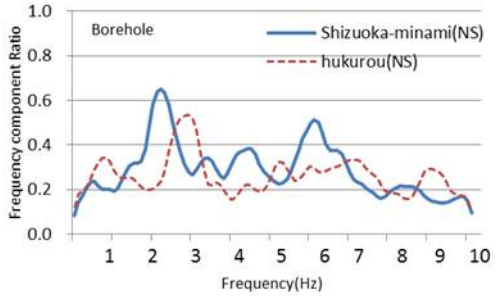

Borehole

Fig. 24 Frequency component ratios of ground motions during Suruga-gulf earthquake in 2009

To compare the distributions of the dominant components, the frequency component ratio is newly introduced as follows.

Frequency component ratio= $F_{RF,MAX}(\omega)/A_{MAX}$

$F_{RF,MAX}(\omega)$: Maximum value of $F_{RF}(\omega;T_j)$; $j=1,2,\cdots M/2$

$M=T/\Delta T$, T ; Duration of the seismic record, ΔT ; Time interval of FFT analysis

$F_{RF}(\omega;T_j)$: Fourier amplitude operated twice of the digital Hanning filter

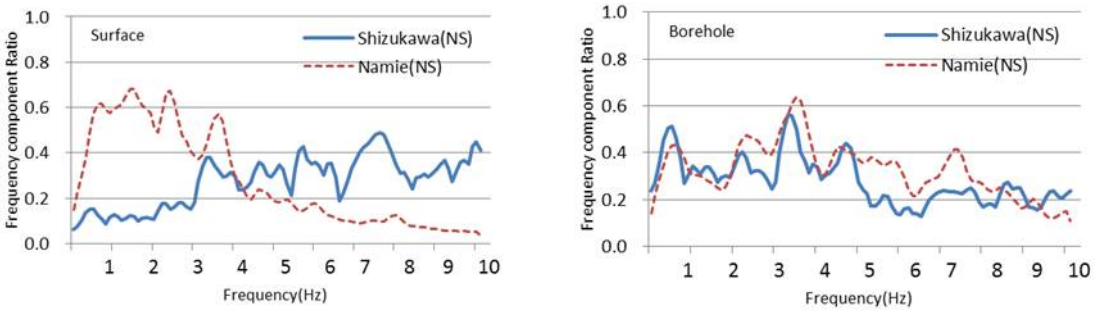

Surface Borehole

Fig. 25 Frequency component ratios during the 2011 off the Pacific coast of Tohoku earthquake

A_{MAX} : Maximum acceleration value of seismic record

(1) Suruga-gulf earthquake in 2009

The frequency component ratio of the NS component is illustrated in Fig. 24. The maximum frequency component ratios of the NS component at the surface are larger than 0.9 and the typical frequency component is amplified. Then the frequency of the maximum value is 2.7 Hz at the Hukuroi and is 3.1 Hz at the Shizuoka-minami.

(2) The 2011 off the Pacific coast of Tohoku earthquake

The frequency component ratio of the NS component is illustrated in Fig. 25. The distributions of the frequency component ratio are different at Shizukawa and Namie. Namely the frequency component ratio at Namie (NS) is amplified in the range less than 4.0 Hz with the value of 0.6. On the other hand, the frequency component ratio at Shizukawa (NS) becomes larger with the increase of frequency with the value of 0.4 as shown in Fig. 25.

3.5 Influence of multi-faults

As shown in Fig. 20, the duration time of the seismic records during the 2011 off Pacific coast of Tohoku earthquake is over two minutes, which is related to the multi-faults. The seismic records at Shizukawa have been separated due to two main shocks. On the other hand, the seismic records at Namie have one main shock with a duration time of 160 seconds.

Therefore the seismic records are divided into two parts as shown in Fig. 20 and they are individually analyzed by the non-stationary Fourier spectra to evaluate the difference in the first and second parts of the seismic records (see Figs. 26 and 27).

(1) Seismic records at Shizukawa

The frequency component ratio at the surface of the NS component becomes larger with the increase of frequency and the frequency component ratio at the surface of the EW and UD components is uniformly distributed in all frequency range with the value less than 0.3 as shown in Fig. 26. The frequency component ratio of the second half is larger than that of the first half in the lower frequency range.

(2)Seismic records at Namie

The analytical result of the EW component is illustrated in Fig. 27. At the surface, the second half has many dominant components in the frequency range less than 5 Hz with the value around 0.6 and the second half has a dominant component with a value of 0.97 at the frequency of 0.9 Hz.

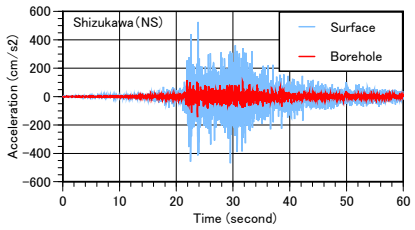

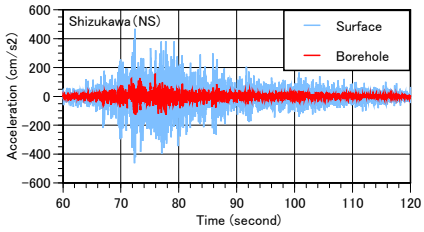

Acceleration profile of Shizukawa (NS) 2011 (Surface and Borehole)

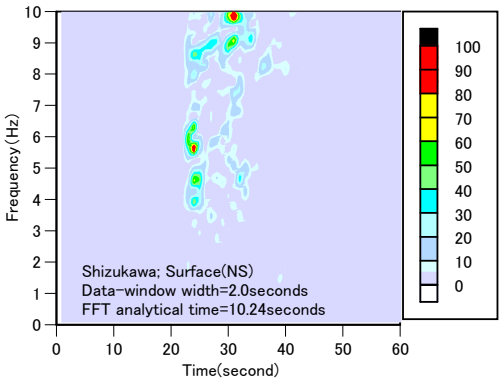

First main-shock (Surface)

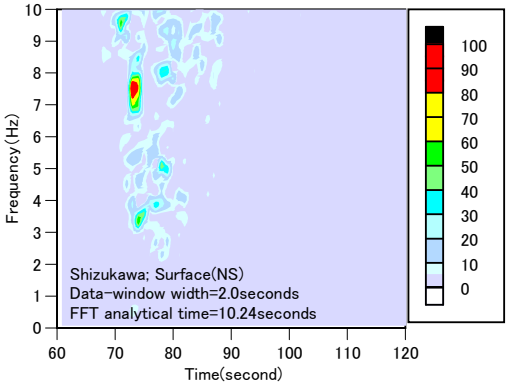

Second main-shock (Surface)

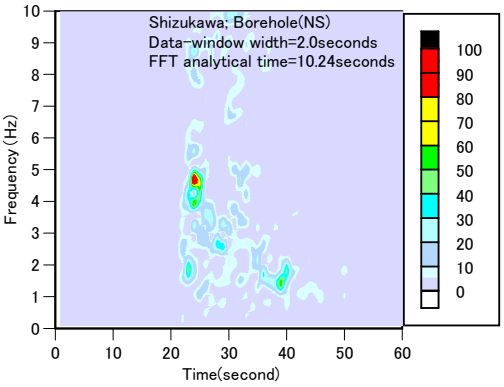

First main-shock (Borehole)

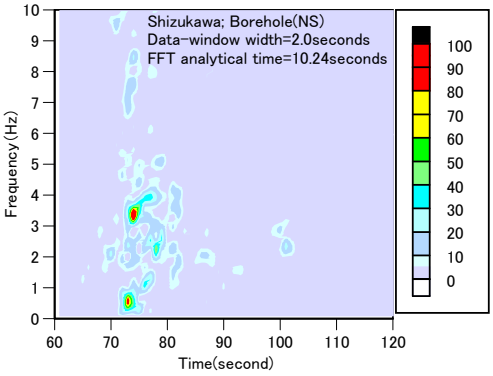

Second main-shock (Borehole)

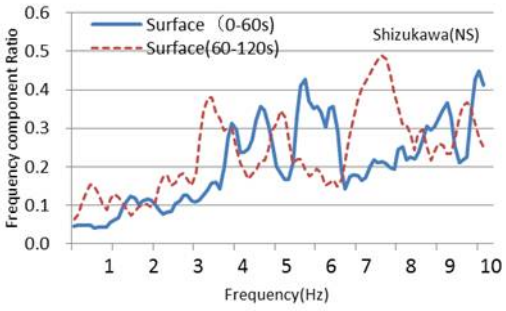

Surface

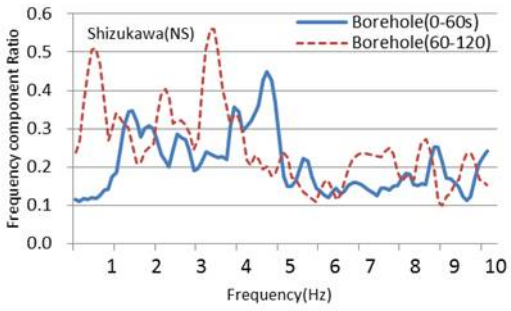

Borehole

Fig. 26 Dominant frequency components of first and second faults in Shizukawa (NS) during the 2011 off the Pacific coast of Tohoku earthquake

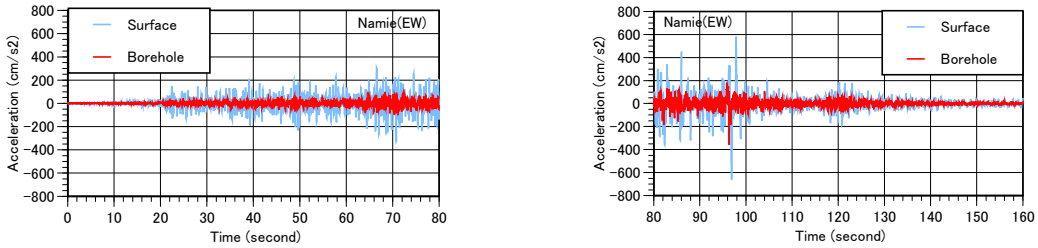

Acceleration profile at Namie (EW) (surface and borehole) during the 2011 off the Pacific coast of Tohoku earthquake

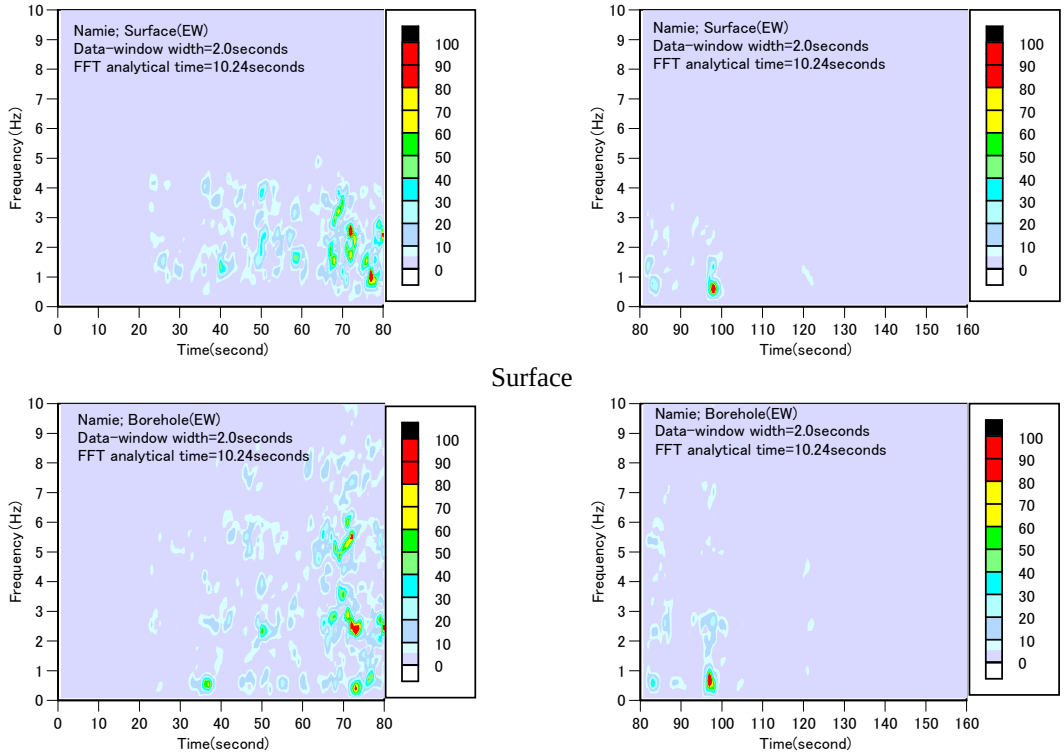

Surface

Borehole

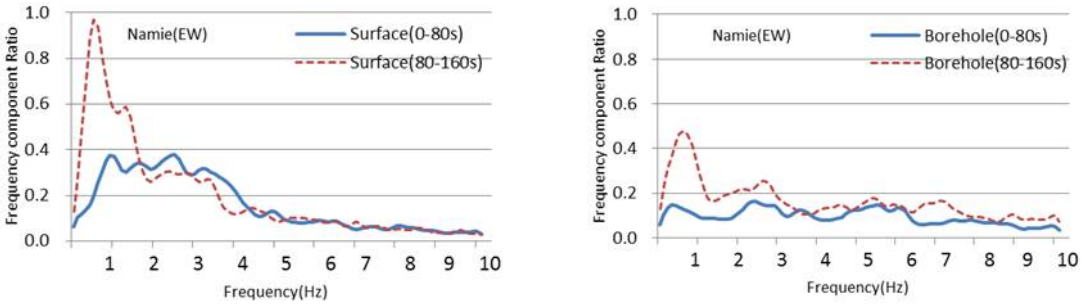

Surface Borehole

Fig. 27 Freguency component ratios of first and second main shocks during the 2011 off the Pacific coast of Tohoku earthquake

The frequency component ratio in the second half is larger than that in the first half in all the frequency ranges.

3.6 Influence of soil property

In the Japanese seismic design code (see Fig. 28), the seismic design force depends on soil conditions. From a view point of soil properties, three sites have been selected, namely Namie as a soft soil site (the third class), Shizuoka-minami as a moderate soil site (the second class) and Shizukawa as a hard rock site (the first class) as shown in the profile of shear wave velocity (see Fig. 29).

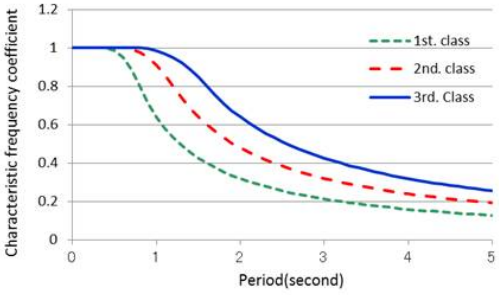

Fig. 28 Seismic design force

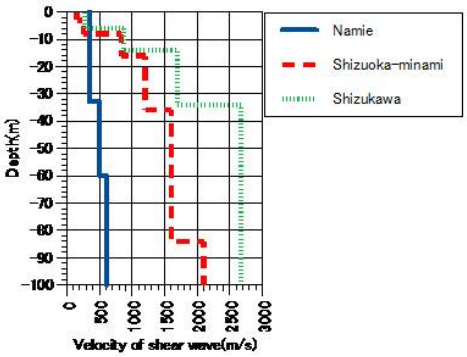

Fig. 29 Velocity of shear wave

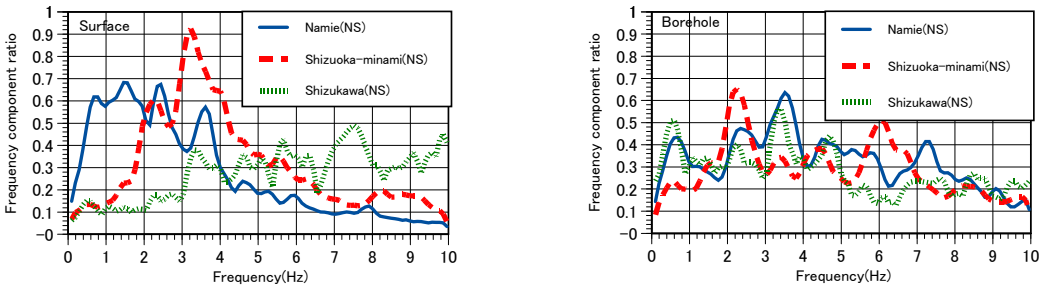

Surface Borehole

Fig. 30 Frequency component ratios at Shizuoka-minami 2009, Namie 2011 and Shizukawa 2011

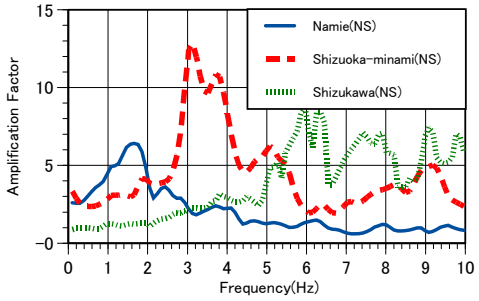

Fig. 31 Amplification factors at Shizuoka-minami 2009, Namie 2011 and Shizukawa 2011

The frequency range of the dominant amplification factor depends on the soil condition, i.e., the soft soil amplifies the acceleration in the low frequency range and the hard rock amplifies the acceleration in the high frequency range as shown in Fig. 30. The influence of the soil condition is evident in the surface frequency component ratio.

As for the amplification factor, the shapes of distribution at the surface are different in three seismic records as shown in Fig. 31. In other words, while the distributions in the borehole are similar in three seismic records, the frequency of dominant component is dependent on the soil condition.

3.7 Comparison of amplification factor and frequency component ratio

As for the amplification factor and the frequency component ratio, the relation between the maximum value and the frequency of its occurrence has been compared in the Fig. 32. The values of maximum frequency ratios of the NS and EW components at Namie are beyond 0.6 and the occurrence frequency is less than 2 Hz.

The maximum frequency component ratio of the NS and EW components at Shizuoka-minami is beyond 0.8 and the occurrence frequency is almost 3 Hz. On the other hand, the maximum frequency component ratio of the NS and EW components at Shizukawa is below 0.5 and the occurrence frequency is almost 7.5 Hz. Furthermore the maximum frequency component ratio of the UD component is less than 0.6 and the occurrence frequency is less than 5 Hz.

The occurrence frequency of the maximum frequency component ratio is clarified by the seismic record, i.e., the occurrence frequency at Namie is the lower frequency, that of Shizuoka-minami is the middle frequency and that of Shizukawa is the higher frequency.

The maximum amplification factor is not clarified for three seismic records.

3.8 Occurrence mechanism of pulse wave

From the results of seismic records, three typical pulse waves have been selected to make clear the occurrence mechanism of pulse waves.

(1) Addition of higher mode at Shizuoka-minami (UD) 2009

The characteristics of pulse waves are as follows (see Fig. 33).

Fig. 32 Relation of frequency component ratio and amplification factor among Namie 2011, Shizuoka-minami 2009 and Shizukawa 2011

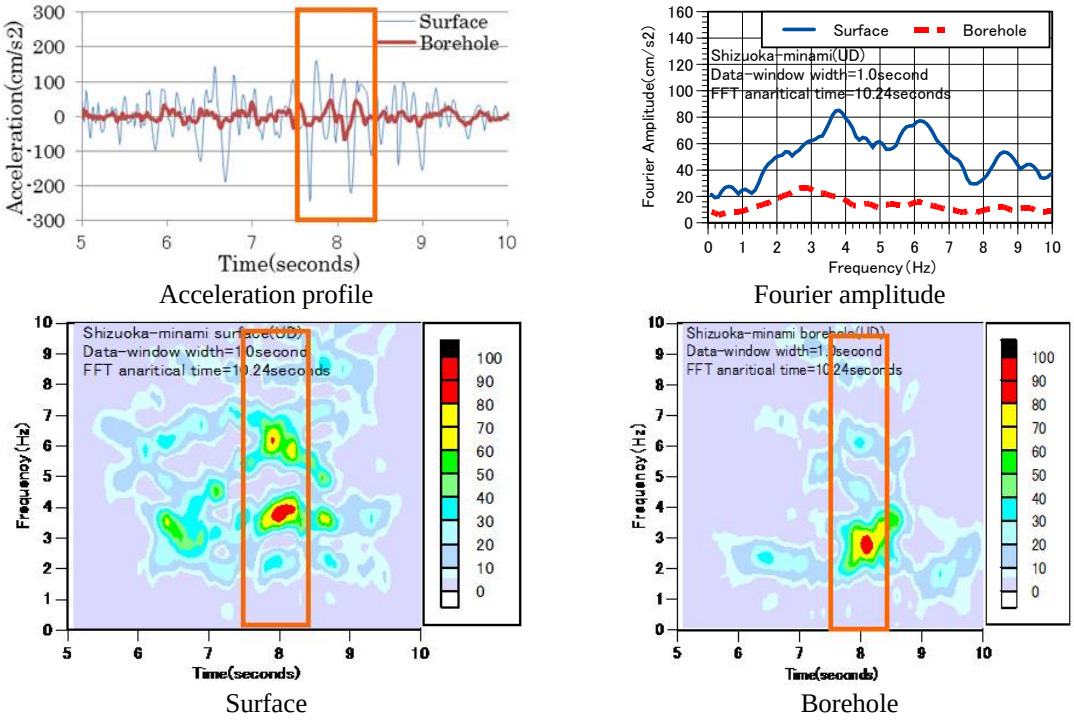

Fig. 33 Acceleration profile, Fourier amplitude and non-stationary Fourier spectra at Shizuoka-minami (UD) during Suruga-gulf earthquake in 2009

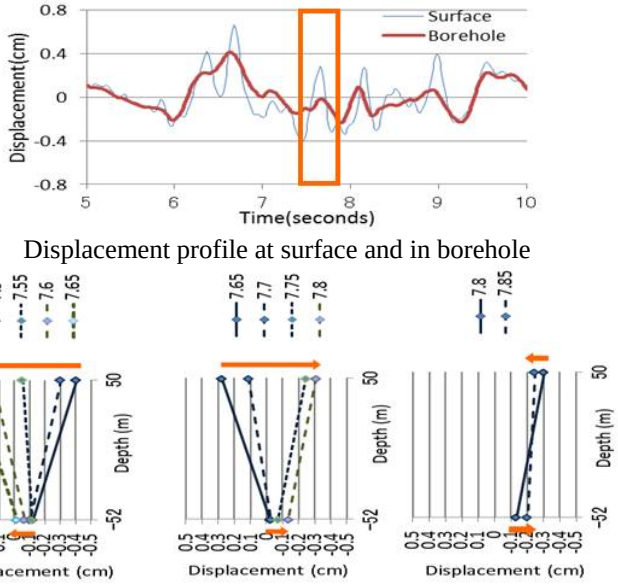

Fig. 34 Displacement profile at surface and in borehole and deformation of surface soil (from 7.45 s to 7.85 s) at Shizuoka-minami during Suruga-gulf earthquake in 2009

(a) The maximum value of the acceleration occurs around 8 seconds.
(b) The frequency of the dominant component is 3.8 Hz and 6.2 Hz.
(c) The dual peaks occur at the displacement profile.
The first occurrence mechanism of pulse waves may result from the resonance of the higher mode in the surface soil. The dual peaks are observed before 8 seconds in the displacement profile (see Fig. 34). The deformation profile in the surface soil is illustrated using the displacement of the surface and the borehole with the interval of 0.05 seconds.

(2) Resonance to fundamental mode in the surface soil at Namie (EW) 2011

The characteristics of pulse waves are as follows (see Fig. 35).
(a) The maximum acceleration occurs around 96 seconds in the borehole and around 97 seconds at the surface.
(b) The frequency of the dominat component is 0.9 Hz.
(c) As for the displacement profile, the phase of the borehole proceeds from the phase of the surface.
(d) As for the displacement profile, two cycles with the amplitude of 30 cm are observed and the phase of borehole proceeds from the phase of the surface as shown in Fig. 36.

The second occurrence mechanism of the pulse wave may result from the amplification of the fundamental mode in the surface soil. The deformation profile in the surface soil is illustrated using the displacement at the surface and in the borehole with the interval of 0.1 seconds.

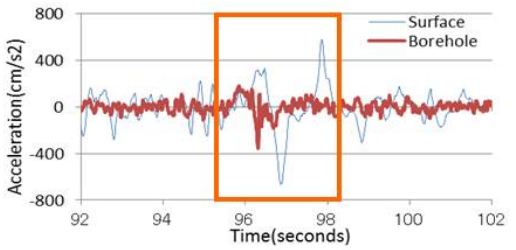

Acceleration profile

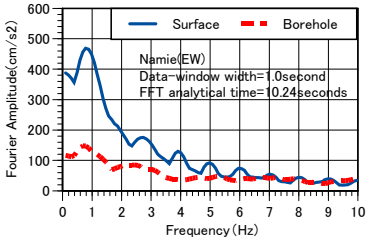

Fourier amplitude

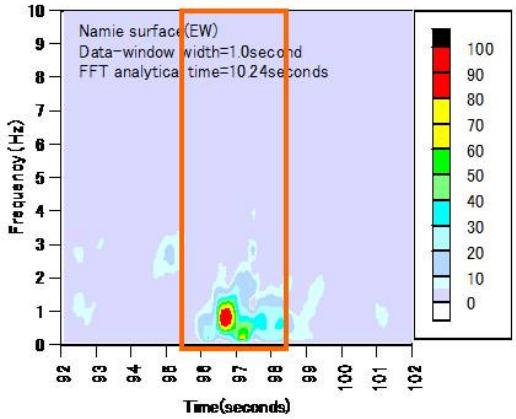

Surface

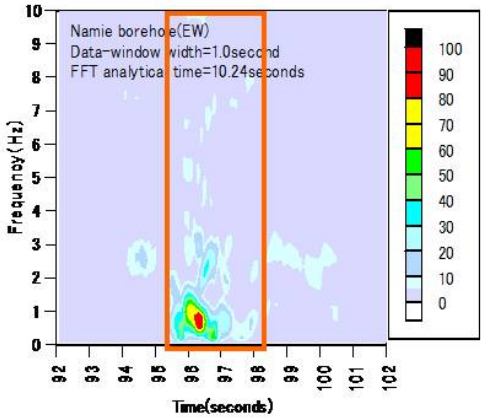

Borehole

Non-stationary Fourier spectra

Fig. 35 Acceleration profile, Fourier amplitude and non-stationary Fourier spectra at Namie (EW) during the 2011 off the Pacific coast of Tohoku earthquake

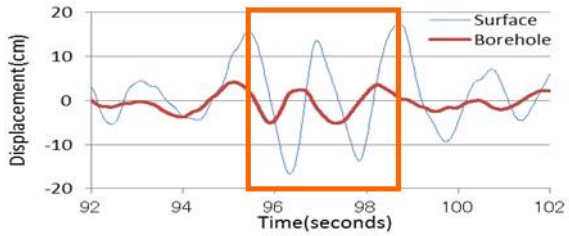

Displacement profile at surface and in borehol

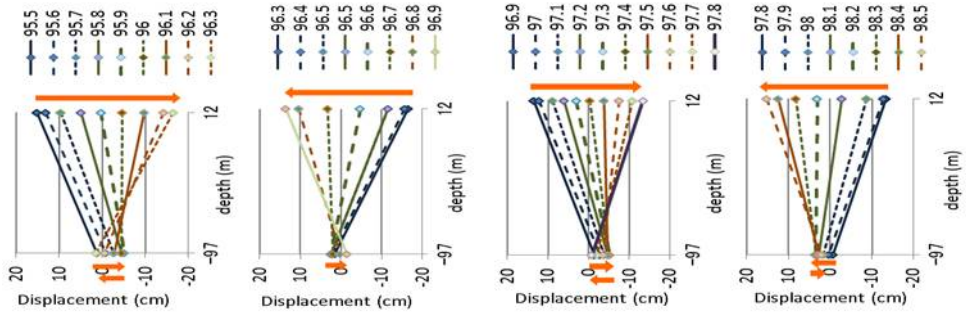

Fig. 36 Displacement profile at surface and in borehole and deformation of surface soil (from 95.5 s to 98.5 s) at Namie (EW) during the 2011 off the Pacific coast of Tohoku earthquake

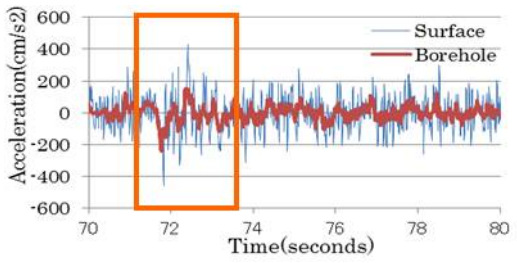

Acceleration profile

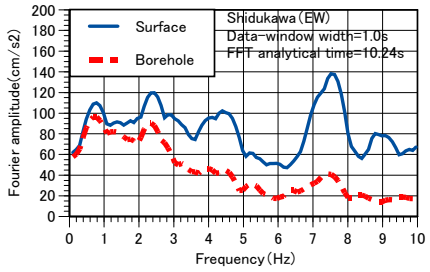

Fourier amplitude

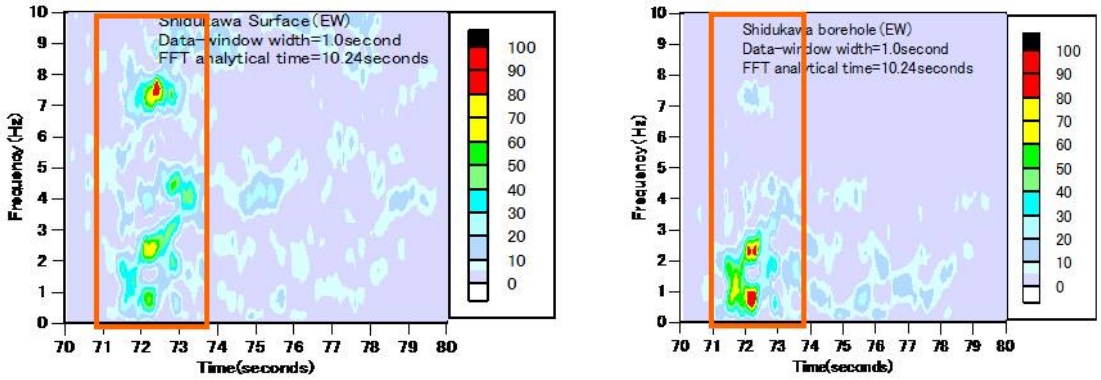

Surface Borehole

Non-stationary Fourier spectra

Fig. 37 Acceleration profile, Fourier amplitude and non-stationary Fourier spectra at Shizukawa (EW) during the 2011 off the Pacific coast of Tohoku earthquake

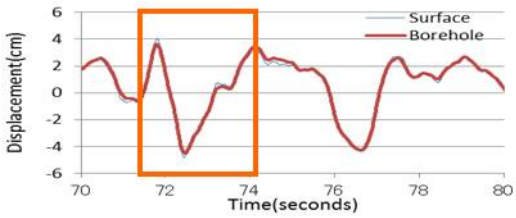

Displacement profile at surface and in borehole

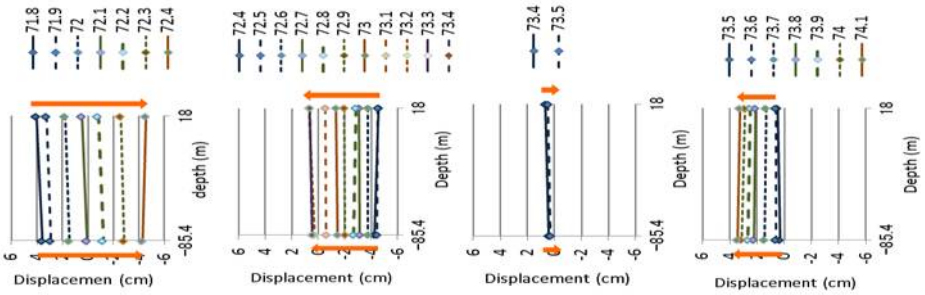

Deformation of surface soil (from 71.8 s to 74.1 s)

Fig. 38 Displacement profile at surface and in borehole and deformation of surface soil (from 71.8 s to 74.1 s) at Shizukawa (EW) during the 2011 off the Pacific coast of Tohoku earthquake

(3) Uniform deformation of surface soil at Shizukawa (EW) 2011

The characteristics of the pulse wave are as follows (see Fig.37).

(a) The maximum acceleration occurs around 72 seconds.

(b) The frequency of the dominat component of the surface is 7.6 Hz.

(c) The displacement profile in the borehole is similar to the displacement profile at the surface.

(d) The deformation of the surface soil shows the uniform movement in the surface soil as shown in Fig. 38.

The third occurrence mechanism of the pulse wave in the acceleration profile may result from the resonance to the higher mode in the surface soil. The deformation profile in the surface soil is illustrated using the displacement at the surface and in the borehole with the interval of 0.1 seconds. This vibration mode is just assumed in the uniform layered soil. The higher modes in the acceleration profile have some influences on the displacement profile.

3.9 Nonlinear behavior in surface soil

From the non-stationary Fourier spectra, the nonlinear behavior is detected, i.e., the deterioration of soil causes the change of the vibration frequency to the lower frequency (see Fig. 39). In the borehole at Shizuoka-minami (NS) 2009, the frequency of the dominant component shifts from 2.5 Hz to 2.0 Hz. At the surface of Shizuoka-minami (EW) 2009, the frequency of dominant component shifts from 4.0 Hz to 3.0 Hz as shown in Fig. 39. This shift occurred during a short time (one or two wave cycles). If the surface wave influenced this frequency change, the duration would be longer.

In the NS component, the maximum value of the amplification factor is 14.9 at the frequency of 3.0 Hz and the value of the amplification factor corresponding to the maximum value of the borehole is 3.8 at the frequency of 2.1 Hz. The local vibration mode is dominant in the surface

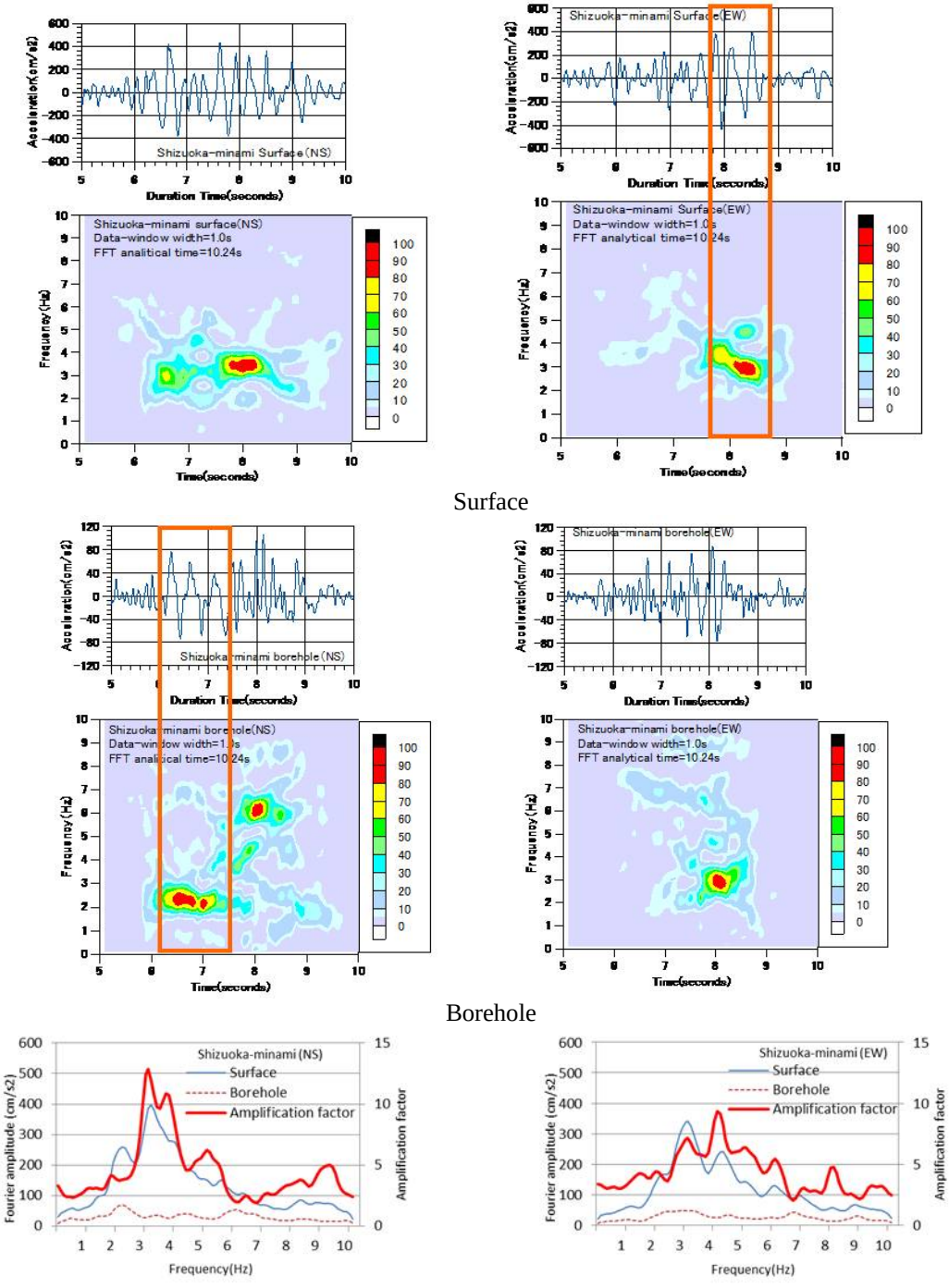

Fig. 39 Non-stationary Fourier spectra, Fourier amplitude and amplification factor during Suruga-gulf earthquake in 2009

soil.

In the EW component, the maximum value of the amplification factor is 8.2 at the frequency of 3.7 Hz and the value of the amplification factor corresponding to the maximum value of the borehole is 5.8 at the frequency of 2.9 Hz. The resonance of the local vibration mode is smaller compared to the NS component.

Furthermore the difference of the dominant component between the surface and the borehole is remarkable, namely the dominant component of the NS component around 6 to 7 seconds is not observed at the EW component and the frequency of dominant component around 8 seconds is different between the NS and EW component.

4. Conclusions

To make clear the occurrence mechanism of the large acceleration in the recent seismic records, the seismic behavior of a building and its surrounding soil has been investigated by means of the non-stationary Fourier spectra and the numerically integrated displacement profile. From the analysis of the seismic records at the Kashiwazaki-Kariwa NPS during the Niigata-ken Chuetsu-oki earthquake in 2007 and the subsequent on-site investigation after the earthquake, the following conclusions have been derived.

(1) The maximum acceleration 680 cm/s^2 at the foundation of the No. 1 unit reactor building is caused by the nonlinear interaction between the building and its surrounding soil.

(2) From the non-stationary Fourier spectra, it has been confirmed that the maximum acceleration is caused by the pulse wave with the frequency 1.2 Hz and the amplitude 470 cm/s^2.

(3) Based on above information, the pulse wave which causes the peak value 680 cm/s^2 can be identified by using the Ricker wavelet.

(4) It has been made clear from the displacement profile that the pulse wave is caused by the second cycle of deformation.

(5) The second cycle of deformation may result from the fact that the restriction of the building is reduced by the gap between the building and its surrounding soil created in the first cycle of deformation.

As for the Suruga-gulf earthquake in 2009 and the 2011 off the Pacific coast of Tohoku earthquake, the seismic records of KiK-net measured at the surface and in the borehole are investigated to evaluate the amplification property of the surface soil.

The concept of frequency component ratio has been newly introduced to compare the distribution shape of the dominant component in the frequency range. Furthermore the amplification factor from the borehole to the surface has been introduced to evaluate the amplification property in the surface soil.

(1) The amplification of the surface soil depends on the soil property.

(2) In the case of the soft soil, a dominant component ratio is amplified by the fundamental mode of the surface soil, i.e., a whipping mode.

(3) In the case of the middle-soft soil, a dominant component ratio is amplified in the lower frequency and the local vibration mode in the surface causes the dual-peak shape in the displacement profile.

(4) In the case of the hard rock, a uniform vibration mode occurs in the displacement profile and the higher frequency mode is induced in the acceleration profile.

(5) Due to the multi-faults, the frequency of the later main shock shifts to a lower frequency range

than the frequency of the first main shock.
(6) From the non-stationary Fourier spectra, it has been confirmed that the frequency of the dominant component shifts to the lower frequency range by the deterioration of the surface soil.

During the 2011 off the Pacific coast of Tohoku earthquake, the maximum accelerations at Tsukidate, Shiogama and Sendai were over 1000 cm/s^2. The acceleration and displacement profiles indicate a mechanical vibration mode, such as a stationary cyclic vibration, and a pulse wave dependent on the maximum displacement (see Appendix-1). The conclusions in this paper have been derived from two representative earthquakes. The applicability of these to other earthquakes should be clarified in the future.

Acknowledgements

The authors thank the Tokyo Electric Power Company. The seismic records of the Kashiwazaki-Kariwa nuclear power station were used to evaluate the interaction between the building and the surrounding soil. The authors also thank the National Research Institute for Earth Science and Disaster Prevention. The seismic records in KiK-net were used to evaluate the amplification property in the surface soil.

References

Chubu Electric Power Company (2009), *Observed seismic records on the Suruga-gulf earthquake in 2009*, September 18th 2009 (in Japanese), (http://www.nisa.meti.go.jp/shingikai/107/3/035/sankou35-1.pdf), (http://www.meti.go.jp/committee/materials/downloadfiles/g71012a07j.pdf).

Japan Association for Earthquake Engineering (2002), *Strong motion records*, (http://www.jaee.gr.jp/en/strong-motion-data/)

Japan Nuclear Energy Safety Organization (2008), "Analysis of seismic motion occurred at Kashiwazaki-Kariwa nuclear power station in the Niigata-ken Chuetsu-oki earthquake 2007", *Investigation Advisory Board of Seismic Safety*, (http://www.meti.go.jp/committee/materials/downloadfiles/g80522a23j.pdf).

Japan Nuclear Energy Safety Organization (2009), *Analysis of seismic records to evaluate the interaction between the building and the surrounding soil*, JNES/SSD09-004 (in Japanese), (http://www.jnes.go.jp/content/000016346.pdf).

Jayaram, N., Baker, J., Okano, H., Ishida, H., McCann Jr., M.W. and Mihara, Y. (2011), "Correlation of response spectral values in Japanese ground motions", *Earthq. Struct.*, **2**(4), 357-376.

Kamae, K., Kawabe, H. and Irikura, K. (2004), "Strong ground motion prediction for huge subduction earthquake using characterized source model and several simulation techniques", *Proc of the 13th WCEE*, Vancouver.

Kamagata, S. (2009), "Non-stationary property of Niigata-ken Chuetsu-oki earthquake on Kashiwazaki-Kariwa nuclear power plants (Occurrence mechanism of Pulse-like wave)", *Abstract of the annual meeting of Architectural Institute of Japan* (in Japanese).

Kamagata, S. (1991), "Non-stationary spectra for seismic response control", *News & Topics Research & Development Structural Engineering (KRCEE0019111501), Kobori Research Complex 1991* (in Japanese).

Nuclear Safety Commission of Japan (2012), "Guideline of seismic design for nuclear power reactor facilities (revised version, draft)", March 14, (in Japanese) (http://www.nsc.go.jp/senmon/shidai/genkishi/genkishi020/siryo2.pdf).

Tahghighi, H. (2011), "Earthquake fault-induced surface rupture- A hybrid strong ground motion simulation technique and discussion for structural design", *Earthq. Eng. Struct. D.*, **40**(14), 1591-1608.
Takabatake, H. and Matsuoka, M. (2012), "Origin of the anomalously large upward acceleration associated with the 2008 Iwate-Miyagi Nairiku earthquake", *Earthq. Struct.*, **3**(5), 675-694.
Takewaki, I., Murakami, S., Fujita, K., Yoshitomi, S. and Tsuji, M. (2011), "The 2011 off the Pacific coast of Tohoku earthquake and response of high-rise buildings under long-period ground motions", *Soil Dyn. Earthq. Eng.,* **31**(11), 1511-1528.
Takewaki, I. (2011), "Preliminary report of the 2011 off the Pacific coast of Tohoku earthquake", *J. Zhejiang University SCIENCE A*, **12**(5), 327-334.
Tokyo Electric Power Company (2007), "First report on the analysis of seismic records measured at Kashiwazaki-Kariwa nuclear power station on the Niigata-ken Chuetsu-oki earthquake 2007", *press-release* (in Japanese), (http://www.tepco.co.jp/cc/press/betu07_j/images/070730d.pdf).
Tokyo Electric Power Company (2008), "Research on the seismic safety of the Kashiwazaki-Kariwa nuclear power station for the Niigata-ken Chuetsu-oki earthquake in 2007", *Investigation Advisory Board of Seismic Safety* (in Japanese), (http://www.meti.go.jp/committee/materials/downloadfiles/g80215b03j.pdf).
Tothong, P. and Cornell, A. (2008), "Structural performance assessment under near-source pulse-like ground motion using advanced ground motion intensity measures", *Earthq. Eng. Struct. D.*, **37**(7), 1013-1037.
Trifunac, M.D. (1971), "Response envelope spectrum and interpretation of strong earthquake ground motion", *B. Seismol. Soc. Am*., **61**(2), 342-356.
Yamada, M., Mori, J. and Heaton, T. (2009), "The slap down phase in high-acceleration records of large earthquakes", *Seismol. Res. Lett*., **80**(4), 559-564.
Yamada, M., Mori, J. and Ohmi, S. (2010), "Temporal changes of subsurface velocities during strong shaking as seen from seismic interferometry", *J. Geophys. Res*., **115**(B3), 302, doi;10,1029/ 2009JB006567,2010.
Yang, D., Pan, J. and Li, G. (2009), "Non-structure-specific intensity measure parameters and characteristic period of near-fault ground motion", *Earthq. Eng. Struct. D*., **38**(11), 1257-1280.

CC

Appendix.1 Seismic records with the maximum acceleration over 1000 cm/s^2

Several seismic records with the maximum acceleration over 1000 cm/s^2 were measured during the 2011 off the Pacific coast of Tohoku earthquake. The K-NET seismic records at two sites were investigated (see Fig. A1.1). The maximum accelerations are listed in Table A1.1.

Fig. A1.2 presents the acceleration and displacement profiles at Tsukidate (NS) and Shiogama (EW). The displacement profile at Tsukidate (NS) indicates a few cycles of stationary vibration mode related to the maximum amplitude of the acceleration record. Regarding Shiogama (EW), the occurrence time of pulse waves in the acceleration profile coincides with that of the negative maximum amplitude of the displacement profile. The shape of the pulse wave seems to be created by the some mechanical vibration mode.

Fig. A1.3 shows non-stationary Fourier spectra and Fourier amplitudes. As for the dominant component of Tsukidate (NS), the frequency is 4.1 Hz and the Fourier amplitude is 1700 cm/s^2. The dominant components have an inclination to shift to the higher frequency. As for the dominant component of Shiogama (EW), the dominant frequency is 2.3 Hz and the amplitude is 520 cm/s^2. It may be concluded that the maximum value of the seismic records results from the non-natural phenomena.

Fig. A1.1 Location of hypocenter and measurement sites (Produced using Google Maps API (http://www5.ocn.ne.jp/~botan/map_g.html))

Table A1.1 Maximum accelerations (cm/s^2)

	NS	EW	UD
Tsukidate	2699.766	1268.536	1879.965
Shiogama	758.598	1969.225	500.76

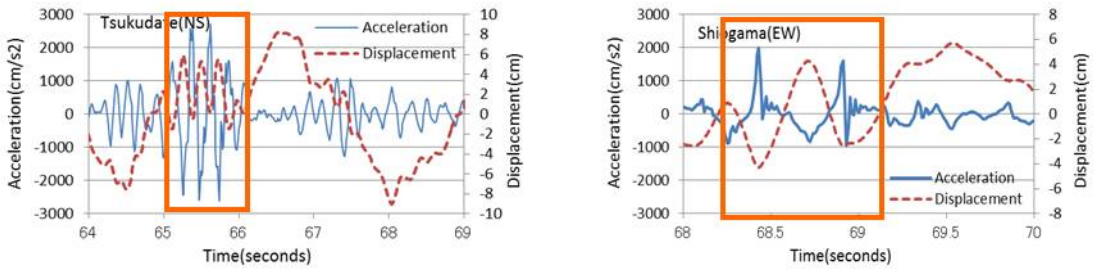

Tsukidate (NS) Shiogama (EW)

Fig. A1.2 Acceleration and displacement profiles

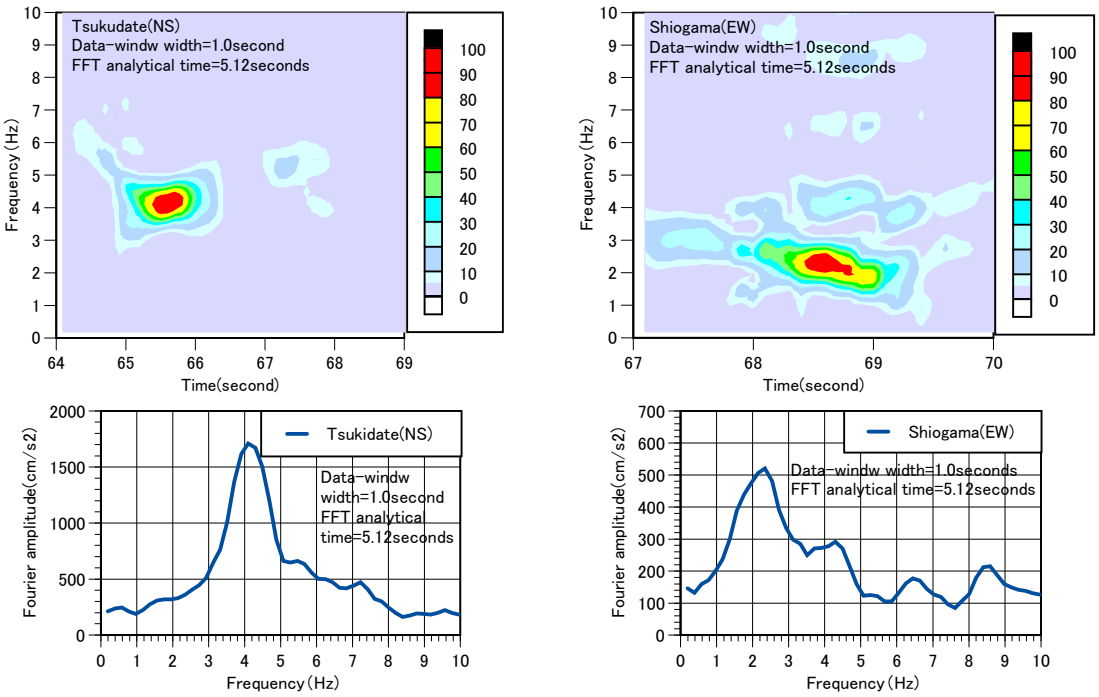

Tsukidate (NS) Shiogama (EW)

Fig. A1.3 Non-stationary Fourier spectra and Fourier amplitudes